Optimal Estimation of Spherical Harmonic Components from a Sample with Spatially Nonuniform Covariance Statistics

KWANG-Y. KIM AND GERALD R. NORTH

Climate System Research Program, Texas A&M University, College Station, Texas

SAMUEL S. SHEN

Department of Mathematics, University of Alberta, Edmonton, Alberta, Canada

(Manuscript received 1 November 1994, in final form 18 September 1995)

ABSTRACT

An optimal estimation technique is presented to estimate spherical harmonic coefficients. This technique is based on the minimization of the mean square error. This optimal estimation technique consists of computing optimal weights for a given network of sampling points. Empirical orthogonal functions (EOFs) are an essential ingredient in formulating the estimation technique of the field of which the second-moment statistics are nonuniform over the sphere. The EOFs are computed using the United Kingdom dataset of global gridded temperatures based on station data. The utility of the technique is further demonstrated by computing a set of spherical harmonic coefficients from the 100-yr long surface temperature fluctuations of the United Kingdom dataset. Next, the validity of the mean-square error formulas is tested by actually calculating an ensemble average of mean-square estimation error. Finally, the technique is extended to estimate the amplitudes of the EOFs.

1. Introduction

The spherical harmonic functions are a natural basis for a global field variable on the surface of the earth. This basis set and its applications to general circulation models are very common (for example, Eliasen et al. 1970; Bourke 1974; Bourke et al. 1977; McAvaney et al. 1978; Pitcher et al. 1983; Ramanathan et al. 1983; Williamson and Swarztrauber 1984). As its use is becoming more commonplace, much theoretical work has been conducted on the sampling bias and on efficient algorithms for computing the spherical harmonic functions and expansion coefficients (Ellsaesser 1966; Orszag 1970; Bourke 1974; McAvaney et al. 1978). These studies mainly deal with identifying a suitable quadrature method and the associated quadrature points and weights.

For historical reasons, however, we do not have the freedom of choosing quadrature points. Instead, we have to rely on whatever data are available on a very sparse, irregular network of sampling points. This introduces potentially significant sampling error in computing the spherical harmonic components, the global average being one component, of a global field and has been a concern for a long time. This also raises a question as to the efficiency of an estimator. Recent studies on estimating the global average temperature include Vinnikov et al. (1990), Trenberth and Olson (1992), North et al. (1992), Hardin and Upson (1993), Madden et al. (1993), and Shen et al. (1994). In this paper, we examine two questions. 1) How large is the sampling error due to an imperfect sampling network in estimating the spherical harmonic coefficients? 2) How do we formulate an estimation technique that minimizes the sampling error?

To minimize the estimation error for a given number of gauges, we can proceed in two distinct directions: 1) We find the best gauge locations or 2) we find the best averaging scheme for fixed gauge locations. The former approach for estimating the global average temperature includes studies by North et al. (1992) and Hardin et al. (1992). In this study, we take the latter approach.

Two key concepts of the linear estimation–sampling theory to be developed here are the optimal weighting and the minimum mean-square error. For a given network, we will formulate a weighted estimator for a spherical harmonic component, which minimizes the error squared in an ensemble sense. The idea of optimal weighting was introduced earlier by Kagan (1979) and Bell (1982, 1986) and was employed recently by Vinnikov et al. (1990), North et al. (1992), Hardin and Upson (1993), and Shen et al. (1994, 1996) among others. The optimal weights are determined such that the error functional is minimized.

Corresponding author address: Dr. Kwang-Yul Kim, Climate System Research Program, College of Geosciences and Maritime Studies, Texas A&M University, College Station, TX 77843-3150.

This estimation–sampling problem depends crucially upon the covariance structure of the underlying fluctuations of the field variable to be estimated. The magnitude and the length scale of the covariance function should properly be integrated into formulating a set of optimal weights for a network of sampling stations. An essential ingredient in the present study is the spectral representation of the covariance field (Kim and North 1991, 1992, 1993). In this spectral approach, the covariance structure is represented in terms of empirical orthogonal functions (EOFs). These EOFs, by definition, take into account the second-moment statistics (variance and covariance) of any nonhomogenous field. This approach enables us to remove simplifying assumptions such as the homogeneity and isotropy of the covariance field (Vinnikov et al. 1990; Shen et al. 1996). The EOFs used in this study are computed based on the 100-yr (1890–1990) United Kingdom dataset (Jones et al. 1986a,b; Woodruff et al. 1987). Details on these EOFs are found in Kim and North (1993) and will not be repeated here.

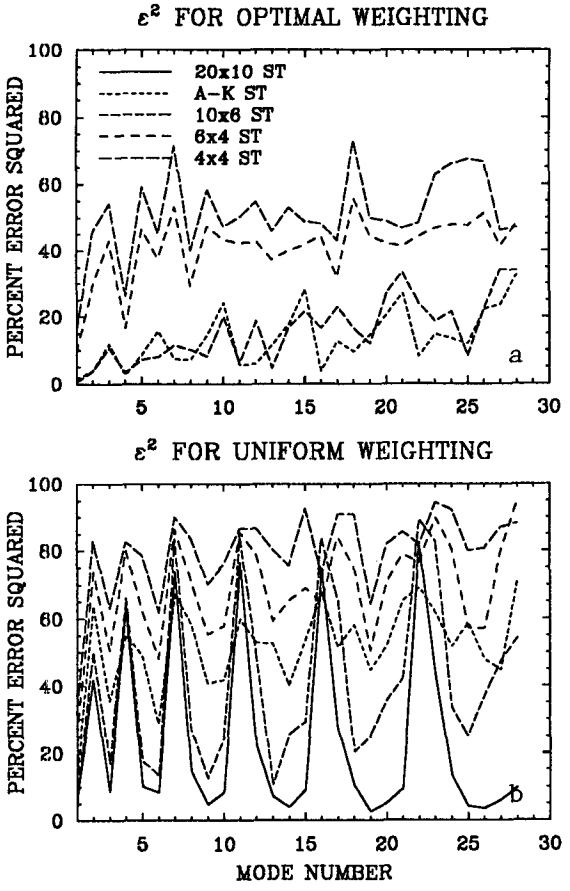

FIG. 1. Percent sampling error squared for four regular networks (20 × 10, 10 × 6, 6 × 4, 4 × 4) and for the Angell–Korshover network: (a) optimal weighting scheme, (b) uniform weighting scheme. The curve for the 20 × 10 case in (a) is right on the abscissa.

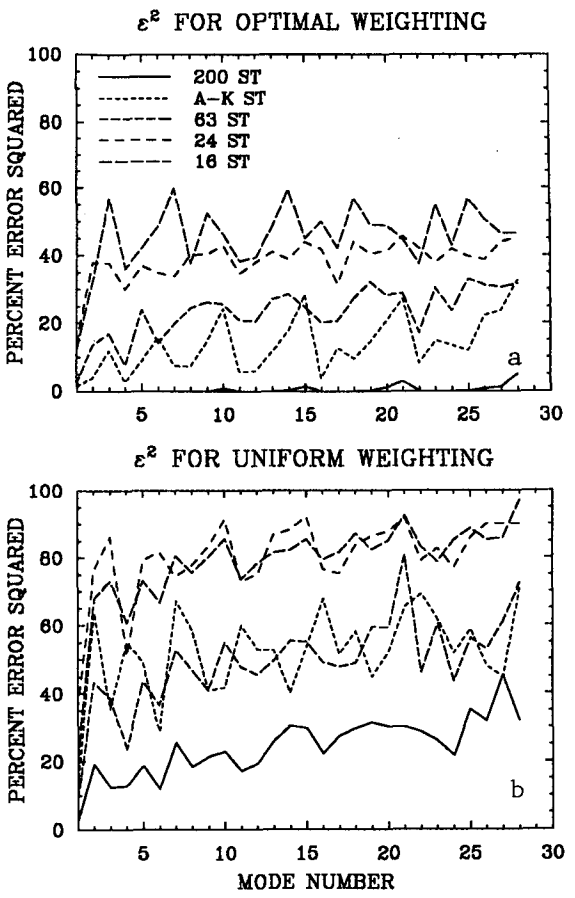

FIG. 2. Percent sampling error squared for four irregular networks (200, 63, 24, 16 points) and for the Angell–Korshover network: (a) optimal weighting scheme, (b) uniform weighting scheme. An irregular network is generated by randomly selecting sampling points with a minimum distance constraint of about 7°.

Finally, the spectral representation of the EOFs allows us to apply the present formulation to the estimation of the EOF amplitude. We will present the formulas for the optimal weights and the ensemble average of error squared for the amplitude of EOFs.

2. Methods

a. Weighted estimator

Expansion coefficients of a global variable, say surface temperature anomalies, in terms of the spherical harmonic basis set are determined by

$$T_{lm}(t) = \int_{4\pi} T(\mathbf{r}, t) Y^*_{lm}(\mathbf{r}) d\Omega, \qquad (1)$$

where $\mathbf{r}$ is a radial unit vector scaled by the earth's radius representing a point on the sphere, $d\Omega$ is the surface area element, 4π is total solid angle, $T(\mathbf{r}, t)$ is a time-dependent field variable, $T_{lm}(t)$ is the time-

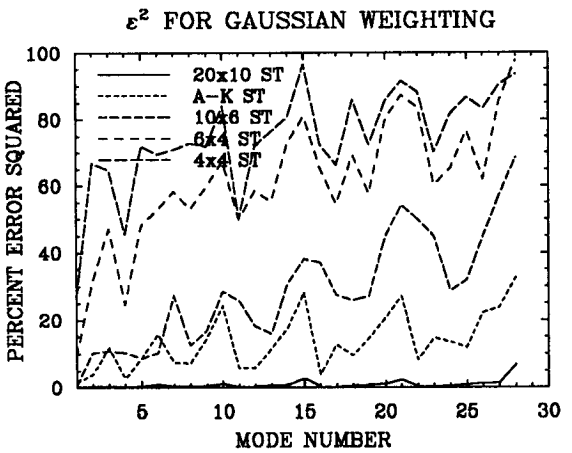

FIG. 3. Percent sampling error squared for four Gaussian networks (20×10, 10×6, 6×4, 4×4). The Gaussian gauges are at Gaussian points in the meridional direction and are uniform in the zonal direction. The weights are Gaussian weights scaled such that $\Sigma\, w_j = 4\pi$. Optimal weighting on the Angell–Korshover network is plotted for a comparison purpose.

dependent expansion coefficient, and $Y_{lm}(\mathbf{r})$ is the spherical harmonic function with order l and rank m. See Arfken (1985) for details on the spherical harmonic functions. Then the field variable is expressed as

$$T(\mathbf{r}, t) = \sum_{l=0}^{\infty} \sum_{m=-l}^{l} T_{lm}(t) Y_{lm}(\mathbf{r}). \tag{2}$$

In practice, the maximum order of expansion is set to a finite value L.

Normally, (1) is evaluated using a Gaussian quadrature method (e.g., Ellsaesser 1966; Orszag 1970; Bourke 1974; McAvaney et al. 1978). To use the Gaussian quadrature method, however, we should first interpolate the field data to the quadrature points. Looking back on the history of sampling stations, most had been purposely established in or near cities, agricultural sites, and airports. Certainly, the station distribution is not ideal for research purposes. The estimation of the spherical harmonic coefficients is affected by the quadrature method used and, in particular, by interpolation error. Here we explore a different approach based on the minimization of the mean-square error of estimation. Given sampling locations, this technique utilizes the global covariance information to calculate an optimal set of weights for averaging given samples.

Let us consider an estimate, $\hat{T}_{lm}$, in the form

$$\hat{T}_{lm}(t) = \sum_{j=1}^{N_{\text{net}}} w_j T(\mathbf{r}_j, t) Y^*_{lm}(\mathbf{r}_j), \tag{3}$$

where

$$\sum_{j=1}^{N_{\text{net}}} w_j = 4\pi. \tag{4}$$

Equation (3) is a quadrature form of (1) for given quadrature points $\{\mathbf{r}_j \mid j = 1, \cdots, N_{\text{net}}\}$. The quadrature weights w_j will be determined based on the minimization of mean-square error. Equation (3) is recast as

$$\hat{T}_{lm}(t) = \int_{4\pi} w_{\text{net}}(\mathbf{r}) T(\mathbf{r}, t) Y^*_{lm}(\mathbf{r}) d\Omega, \tag{5}$$

where

$$w_{\text{net}}(\mathbf{r}) = \sum_{j=1}^{N_{\text{net}}} w_j \delta(\mathbf{r} - \mathbf{r}_j). \tag{6}$$

From (2) and (5), we can derive an expression for the aliasing of a spectral component. Namely,

$$\begin{aligned} \hat{T}_{lm}(t) &= \int_{4\pi} w_{\text{net}}(\mathbf{r}) Y^*_{lm}(\mathbf{r}) \sum_{l',m'} T_{l'm'}(t) Y_{l'm'} d\Omega \\ &= \sum_{l',m'} \Big[\sum_{j=1}^{N_{\text{net}}} w_j Y^*_{lm}(\mathbf{r}_j) Y_{l'm'}(\mathbf{r}_j) \Big] T_{l'm'}(t) \\ &= \sum_{l',m'} A_{lm;l'm'} T_{l'm'}(t). \end{aligned} \tag{7}$$

The matrix A is called the aliasing matrix and its structure shows how different spectral components contribute to the aliasing of the estimate $\hat{T}_{lm}$. For the anomaly fields, however, $\langle T_{lm} \rangle = 0$ and hence $\langle \hat{T}_{lm} \rangle = 0$, where $\langle\ \rangle$ represents an ensemble average. The anomaly is with respect to the ensemble average and an ensemble average may be taken as an average over a long time interval for practical reasons. Aliasing and bias, therefore, is not an issue for the anomaly fields. For $\langle T_{lm} \rangle \neq 0$, as in the case of the observed surface temperature field with a linear trend, an optimal estimator is in general aliased and biased unless

$$\sum_{j=1}^{N_{\text{net}}} w_j Y^*_{lm}(\mathbf{r}_j) Y_{l'm'}(\mathbf{r}_j) = \delta_{ll'}\delta_{mm'}. \tag{8}$$

This constraint is a quadrature representation of

$$\int_{4\pi} Y^*_{lm}(\mathbf{r}) Y_{l'm'}(\mathbf{r}) d\Omega = \delta_{ll'}\delta_{mm'}, \tag{9}$$

where each weight is the areal element associated with a quadrature point. Although (4) does not guarantee (8) to hold, it is introduced to properly constrain this integration. Of course, the mean-square error would be smaller at the risk of unconstrained alias if this condition is removed.

b. Minimum mean-square error

The mean-squared error of the estimator $\hat{T}_{lm}(t)$ is defined as

TABLE 1. Percent sampling error squared (theoretical values in parenthesis) obtained from the 100-yr (1890–1990) United Kingdom data (Jones et al. 1986a,b; Woodruff et al. 1987). Three different estimation techniques (optimal, uniform, and Gaussian weighting schemes) were applied to four regular networks. The optimal and uniform techniques were applied also to the Angell–Korshover network.

		Spherical harmonic mode number																											
		1	2	3	4	5	6	7	8	9	10	11	12	13	14	15	16	17	18	19	20	21	22	23	24	25	26	27	28
4 × 4	OPT	10	39	53	24	59	43	78	40	56	48	51	52	49	51	49	51	39	75	50	48	47	50	63	69	67	70	44	46
		(16)	(46)	(54)	(26)	(59)	(45)	(71)	(40)	(58)	(47)	(50)	(55)	(46)	(53)	(49)	(48)	(43)	(73)	(50)	(49)	(47)	(49)	(63)	(66)	(67)	(67)	(46)	(47)
	UNF	24	81	63	83	81	57	93	85	70	75	89	87	82	76	95	79	90	91	67	85	84	87	95	91	82	86	89	89
		(33)	(83)	(63)	(83)	(79)	(62)	(90)	(83)	(70)	(76)	(87)	(87)	(80)	(76)	(93)	(73)	(91)	(91)	(64)	(82)	(86)	(82)	(94)	(92)	(80)	(81)	(87)	(88)
	GAUSS	18	59	65	41	74	66	75	76	70	83	50	71	78	81	97	79	61	85	74	88	91	90	70	78	87	87	92	94
		(26)	(67)	(65)	(45)	(72)	(70)	(71)	(73)	(72)	(84)	(50)	(72)	(76)	(81)	(96)	(72)	(66)	(86)	(72)	(86)	(92)	(88)	(70)	(82)	(87)	(83)	(90)	(94)
6 × 4	OPT	5	21	40	15	42	32	55	29	45	43	42	42	38	38	40	50	29	59	44	42	39	42	47	50	48	48	38	47
		(10)	(29)	(43)	(17)	(46)	(37)	(53)	(29)	(47)	(43)	(42)	(43)	(37)	(40)	(42)	(44)	(32)	(56)	(45)	(42)	(41)	(44)	(47)	(48)	(48)	(51)	(41)	(48)
	UNF	18	70	47	81	63	43	89	75	54	56	88	79	63	66	69	73	82	78	50	73	77	82	91	79	59	56	84	97
		(25)	(74)	(50)	(80)	(62)	(48)	(86)	(71)	(55)	(58)	(85)	(79)	(59)	(65)	(69)	(65)	(84)	(75)	(51)	(71)	(79)	(76)	(90)	(80)	(57)	(57)	(80)	(95)
	GAUSS	5	22	44	23	50	46	57	58	61	64	50	57	62	76	82	69	46	74	59	82	87	85	61	64	79	61	90	98
		(9)	(31)	(47)	(25)	(48)	(53)	(58)	(53)	(60)	(67)	(50)	(58)	(55)	(73)	(81)	(65)	(55)	(69)	(58)	(80)	(87)	(84)	(60)	(65)	(77)	(62)	(86)	(98)
10 × 6	OPT	0	2	8	3	8	6	12	10	8	17	4	17	5	16	19	17	17	17	12	24	35	22	18	22	8	21	34	32
		(0)	(4)	(11)	(3)	(7)	(8)	(12)	(10)	(8)	(20)	(6)	(19)	(5)	(17)	(23)	(17)	(23)	(17)	(12)	(27)	(34)	(24)	(19)	(22)	(8)	(23)	(35)	(36)
	UNF	5	42	16	69	19	12	86	29	13	22	86	46	14	26	26	85	58	23	27	32	42	91	82	36	26	39	46	53
		(7)	(50)	(17)	(66)	(18)	(13)	(83)	(27)	(13)	(25)	(84)	(49)	(11)	(26)	(29)	(84)	(65)	(20)	(25)	(36)	(42)	(89)	(83)	(34)	(25)	(37)	(47)	(54)
	GAUSS	0	10	10	9	10	9	33	14	17	27	23	17	22	32	36	39	22	29	28	44	53	50	47	28	35	47	56	69
		(0)	(10)	(11)	(10)	(9)	(10)	(27)	(12)	(17)	(28)	(26)	(18)	(16)	(31)	(38)	(37)	(27)	(26)	(27)	(45)	(54)	(50)	(45)	(29)	(32)	(45)	(57)	(69)
A–K	OPT	1	4	15	3	11	15	15	9	16	28	5	5	15	23	26	5	13	11	15	19	27	9	17	15	14	27	26	34
		(1)	(4)	(12)	(3)	(9)	(16)	(7)	(7)	(15)	(24)	(6)	(6)	(12)	(18)	(28)	(4)	(13)	(10)	(15)	(21)	(28)	(8)	(15)	(13)	(12)	(22)	(24)	(34)
	UNF	9	61	33	54	51	29	72	63	42	45	63	52	57	45	53	65	45	59	45	52	69	67	63	50	58	48	51	77
		(13)	(64)	(35)	(55)	(49)	(29)	(67)	(58)	(41)	(42)	(60)	(53)	(53)	(40)	(54)	(68)	(51)	(58)	(45)	(52)	(66)	(69)	(62)	(52)	(59)	(48)	(45)	(72)
20 × 10	OPT	0	0	0	0	0	0	0	0	0	0	0	0	0	0	0	0	0	0	0	0	0	0	0	0	0	0	0	0
		(0)	(0)	(0)	(0)	(0)	(0)	(0)	(0)	(0)	(0)	(0)	(0)	(0)	(0)	(0)	(0)	(0)	(0)	(0)	(0)	(0)	(0)	(0)	(0)	(0)	(0)	(0)	(0)
	UNF	5	29	9	66	12	8	70	18	5	8	78	22	9	4	9	67	24	11	3	6	10	83	46	11	5	4	6	10
		(7)	(42)	(9)	(63)	(10)	(8)	(74)	(15)	(5)	(8)	(76)	(22)	(7)	(4)	(9)	(75)	(28)	(11)	(3)	(5)	(9)	(82)	(44)	(13)	(4)	(3)	(6)	(10)
	GAUSS	0	0	0	0	0	1	0	0	0	1	0	0	1	1	6	0	0	0	1	2	4	0	0	0	1	2	3	13
		(0)	(0)	(0)	(0)	(0)	(1)	(0)	(0)	(0)	(1)	(0)	(0)	(1)	(1)	(3)	(0)	(0)	(0)	(1)	(1)	(2)	(0)	(0)	(0)	(1)	(1)	(1)	(7)

TABLE 2. Percent sampling error squared (theoretical values in parenthesis) obtained from the 100-yr (1890–1990) United Kingdom data (Jones et al. 1986a,b; Woodruff et al. 1987). The optimal and uniform weighting techniques were applied to four irregular networks and the Angell–Korshover network.

		Spherical harmonic mode number																									
		1	2	3	4	5	6	7	8	9	10	11	12	13	14	15	16	17	18	19	20	21	22	23	24	25	26	27	28
16	OPT	7	30	56	35	42	44	60	38	52	44	39	38	53	59	43	53	37	58	50	47	44	34	57	45	59	50	45	46
		(12)	(32)	(57)	(36)	(42)	(49)	(60)	(38)	(52)	(46)	(38)	(39)	(48)	(59)	(45)	(50)	(42)	(57)	(49)	(49)	(45)	(37)	(55)	(43)	(57)	(51)	(46)	(46)
	UNF	13	63	74	54	75	65	84	77	84	87	78	77	84	85	86	83	78	88	85	88	93	83	79	85	91	88	90	98
		(20)	(68)	(73)	(61)	(73)	(67)	(80)	(76)	(80)	(86)	(74)	(78)	(82)	(82)	(85)	(79)	(82)	(87)	(82)	(85)	(92)	(83)	(79)	(85)	(89)	(85)	(86)	(97)
24	OPT	9	34	38	27	37	31	33	42	39	41	30	39	39	37	44	42	30	43	41	40	43	41	37	40	39	37	46	44
		(14)	(38)	(38)	(30)	(37)	(35)	(34)	(40)	(40)	(43)	(34)	(38)	(41)	(39)	(44)	(42)	(31)	(44)	(40)	(41)	(45)	(42)	(38)	(42)	(40)	(39)	(44)	(45)
	UNF	26	73	89	48	83	83	76	81	86	94	70	78	90	91	94	76	73	87	88	90	93	78	82	79	88	91	93	92
		(35)	(76)	(86)	(51)	(79)	(82)	(74)	(78)	(83)	(91)	(73)	(75)	(87)	(88)	(92)	(77)	(75)	(84)	(86)	(88)	(92)	(79)	(83)	(77)	(86)	(90)	(90)	(90)
63	OPT	1	11	15	6	21	11	19	23	23	23	19	18	28	28	21	21	16	28	31	27	25	14	29	23	35	31	29	27
		(2)	(14)	(17)	(7)	(24)	(14)	(20)	(24)	(26)	(26)	(21)	(20)	(27)	(30)	(25)	(20)	(20)	(27)	(32)	(28)	(29)	(17)	(30)	(24)	(34)	(31)	(31)	(32)
	UNF	5	38	44	20	45	35	55	49	40	58	53	45	58	63	57	51	43	52	66	66	83	46	63	43	58	57	67	74
		(9)	(43)	(39)	(24)	(44)	(37)	(53)	(47)	(41)	(55)	(48)	(46)	(50)	(55)	(55)	(49)	(48)	(49)	(60)	(59)	(81)	(46)	(60)	(43)	(56)	(53)	(61)	(72)
A–K	OPT	1	4	15	3	11	15	15	9	16	28	5	5	15	23	26	5	13	11	15	19	27	9	17	15	14	27	26	34
		(1)	(4)	(12)	(3)	(9)	(16)	(7)	(7)	(15)	(24)	(6)	(6)	(12)	(18)	(28)	(4)	(13)	(10)	(15)	(21)	(28)	(8)	(15)	(13)	(12)	(22)	(24)	(34)
	UNF	9	61	33	54	51	29	72	63	42	45	63	52	57	45	53	65	45	59	45	52	69	67	63	50	58	48	51	77
		(13)	(64)	(35)	(55)	(49)	(29)	(67)	(58)	(41)	(42)	(60)	(53)	(53)	(40)	(54)	(68)	(51)	(58)	(45)	(52)	(66)	(69)	(62)	(52)	(59)	(48)	(45)	(72)
200	OPT	0	0	0	0	0	0	0	0	0	1	0	0	0	0	1	0	0	0	0	1	2	0	0	0	0	1	2	4
		(0)	(0)	(0)	(0)	(0)	(0)	(0)	(0)	(0)	(1)	(0)	(0)	(0)	(0)	(1)	(0)	(0)	(0)	(0)	(1)	(3)	(0)	(0)	(0)	(0)	(1)	(2)	(6)
	UNF	1	13	13	13	20	11	29	22	23	24	13	21	29	35	33	25	27	35	29	30	31	28	27	23	34	28	57	33
		(2)	(19)	(12)	(13)	(19)	(12)	(25)	(18)	(21)	(23)	(17)	(19)	(26)	(30)	(30)	(22)	(27)	(30)	(31)	(30)	(30)	(29)	(26)	(22)	(35)	(32)	(45)	(32)

$$\epsilon_{lm}^2 = \langle |T_{lm} - \hat{T}_{lm}|^2 \rangle = \left\langle \left| \int T(\mathbf{r}) Y_{lm}^*(\mathbf{r}) d\Omega - \int w_{\text{net}}(\mathbf{r}) T(\mathbf{r}) Y_{lm}^*(\mathbf{r}) d\Omega \right|^2 \right\rangle$$

$$= \int d\Omega \int d\Omega' \langle T(\mathbf{r}) T(\mathbf{r}') \rangle \{ Y_{lm}^*(\mathbf{r}) Y_{lm}(\mathbf{r}') - [w_{\text{net}}(\mathbf{r}) + w_{\text{net}}(\mathbf{r}')] Y_{lm}^*(\mathbf{r}) Y_{lm}(\mathbf{r}') + w_{\text{net}}(\mathbf{r}) w_{\text{net}}(\mathbf{r}') Y_{lm}^*(\mathbf{r}) Y_{lm}(\mathbf{r}') \}. \quad (10)$$

The covariance is given by (Kim and North 1993)

$$\langle T(\mathbf{r}) T(\mathbf{r}') \rangle = \sum_n \lambda_n \psi_n(\mathbf{r}) \psi_n(\mathbf{r}'), \quad (11)$$

where $\psi_n(\mathbf{r})$ is the nth eigenfunction and λ_n is the corresponding eigenvalue of the covariance matrix of the global temperature field. Then we can rewrite (10) as

$$\epsilon_{lm}^2 = \sum_n \lambda_n [\psi_{lm}^{(n)} \psi_{lm}^{*(n)} - \psi_{lm}^{*(n)} \sum_j w_j \psi_n(\mathbf{r}_j) Y_{lm}^*(\mathbf{r}_j) - \psi_{lm}^{(n)} \sum_j w_j \psi_n(\mathbf{r}_j) Y_{lm}(\mathbf{r}_j) + \sum_j w_j \psi_n(\mathbf{r}_j) Y_{lm}^*(\mathbf{r}_j) \times \sum_k w_k \psi_n(\mathbf{r}_k) Y_{lm}(\mathbf{r}_k)]. \quad (12)$$

Note that $\psi_{lm}^{(n)}$ is the projection of $\psi_n(\mathbf{r})$ onto the spherical harmonic component $Y_{lm}(\mathbf{r})$.

Now the Lagrangian is

$$J[\mathbf{w}] = \epsilon^2[\mathbf{w}] - 2\Lambda\{\sum w_j - 4\pi\}, \quad (13)$$

where Λ is Lagrange multiplier. An extremum of the Lagrange functional is found by

$$\frac{\partial J}{\partial w_j} = 0, \quad \text{and} \quad \frac{\partial J}{\partial \Lambda} = 0. \quad (14)$$

After some manipulations, we find

$$\sum_n \lambda_n \Re[\psi_n(\mathbf{r}_j) Y_{lm}^*(\mathbf{r}_j) \sum_k w_k \psi_n(\mathbf{r}_k) Y_{lm}(\mathbf{r}_k)] - \Lambda = \sum_n \lambda_n \Re[\psi_{lm}^{*(n)} \psi_n(\mathbf{r}_j) Y_{lm}^*(\mathbf{r}_j)] \quad \text{for } j = 1, \cdots, N_{\text{net}},$$

$$\sum_j w_j = 4\pi. \quad (15)$$

Equation (15) is an $(N_{\text{net}} + 1) \times (N_{\text{net}} + 1)$ matrix equation for unknowns w_j, $j = 1, \cdots, N_{\text{net}}$, and Λ.

Once the optimal weights are determined, minimum mean-square error is given by

$$(\epsilon_{lm}^2)_{\text{opt}} = \sum_n \lambda_n |\psi_{lm}^{(n)} - \sum_j w_j \psi_n(\mathbf{r}_j) Y_{lm}^*(\mathbf{r}_j)|^2, \quad (16)$$

or equivalently,

$$\frac{(\epsilon_{lm}^2)_{\text{opt}}}{\sigma_{lm}^2} = \frac{\sum_n \lambda_n |\psi_{lm}^{(n)} - \sum_j w_j \psi_n(\mathbf{r}_j) Y_{lm}^*(\mathbf{r}_j)|^2}{\sum_n \lambda_n |\psi_{lm}^{(n)}|^2}. \quad (17)$$

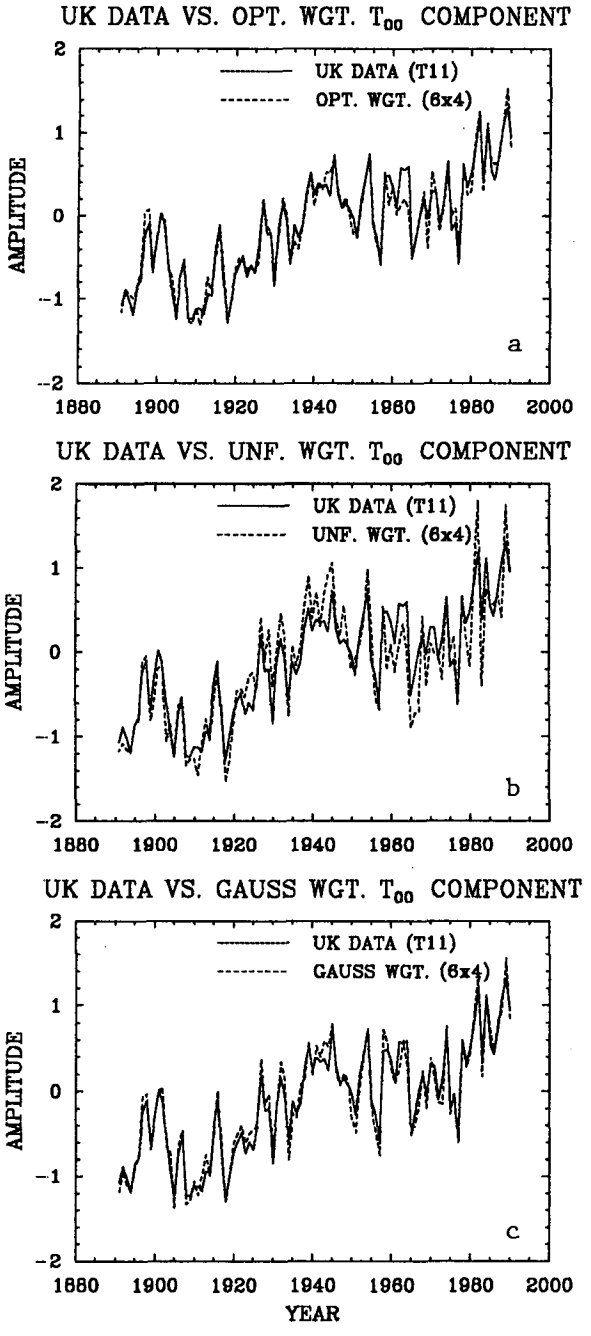

FIG. 4. The 100-yr time series of T_{00} component from the United Kingdom dataset (Jones et al. 1986a,b). The estimation technique is based on a 6 × 4 regular network. Employed weighting schemes are (a) optimal, (b) uniform, and (c) Gaussian. The respective percent sampling errors squared are 5%, 18%, and 5%.

c. *Optimal estimate for EOF amplitude*

The formulation derived above is easily modified for the estimation of the EOF amplitude. We define the amplitude of EOF, $\phi_n(\mathbf{r})$, as

$$A_n(t) = \int_{4\pi} T(\mathbf{r}, t)\phi_n^*(\mathbf{r})d\Omega, \tag{18}$$

where, as in Kim and North (1993),

$$\phi_n(\mathbf{r}) = \sum_{l,m} \phi_{lm}^{(n)} Y_{lm}(\mathbf{r}). \tag{19}$$

The $\{\phi_n(\mathbf{r})\}$ of which the amplitude is to be estimated is not necessarily the same set of EOFs as in the formulation of the optimal estimator. As before, we define a weighted estimate of $A_n(t)$ as

$$\hat{A}_n(t) = \sum_{j=1}^{N_{\text{net}}} w_j T(\mathbf{r}_j, t)\phi_n(\mathbf{r}_j). \tag{20}$$

After similar algebraic manipulations as above, we obtain

$$\sum_l \lambda_l \psi_l(\mathbf{r}_j)\phi_n(\mathbf{r}_j) \sum_k w_k \psi_l(\mathbf{r}_k)\phi_n(\mathbf{r}_k) - \Lambda$$
$$= \sum_l \lambda_l \psi_n^{(l)} \psi_l(\mathbf{r}_j)\phi_n(\mathbf{r}_j) \quad \text{for} \quad j = 1, \cdots, N_{\text{net}},$$
$$\sum_j w_j = 4\pi, \tag{21}$$

where $\psi_n^{(l)}$ is the projection of $\psi_l(\mathbf{r})$ on $\phi_n(\mathbf{r})$. A scaled minimum mean-square error is

$$\frac{(\epsilon_n^2)_{\text{opt}}}{\sigma_n^2} = \frac{\sum_l \lambda_l |\psi_n^{(l)} - \sum_j w_j \psi_l(\mathbf{r}_j)\phi_n(\mathbf{r}_j)|^2}{\sum_l \lambda_l |\psi_n^{(l)}|^2}. \tag{22}$$

For the special case of $\phi(\mathbf{r}) = \psi(\mathbf{r})$,

$$\sum_l \lambda_l \psi_l(\mathbf{r}_j)\psi_n(\mathbf{r}_j) \sum_k w_k \psi_l(\mathbf{r}_k)\psi_n(\mathbf{r}_k) - \Lambda$$
$$= \lambda_n \psi_n^2(\mathbf{r}_j) \quad \text{for} \quad j = 1, \cdots, N_{\text{net}}, \tag{23}$$

and the minimum mean-square error is

$$\frac{(\epsilon_n^2)_{\text{opt}}}{\lambda_n} = 1 - 2\sum_j w_j \psi_n^2(\mathbf{r}_j)$$
$$+ \sum_l \frac{\lambda_l}{\lambda_n} [\sum_j w_j \psi_l(\mathbf{r}_j)\psi_n(\mathbf{r}_j)]^2. \tag{24}$$

3. Results and discussion

Throughout the discussion, percent sampling error squared is used as a measure of the accuracy of an estimation technique. The percent sampling error squared is defined by $\epsilon_{lm}^2/(\sigma_{lm}^2 + \epsilon_{lm}^2) \times 100\%$. When ϵ^2 is much bigger than σ^2, the percent sampling error squared approaches 100%, while it becomes zero if ϵ^2 is much smaller than σ^2.

Figure 1 shows the percent sampling error squared for four different regular networks and for the Angell–Korshover (A–K) network (Angell and Korshover 1983). For the uniform weighting case, we simply use

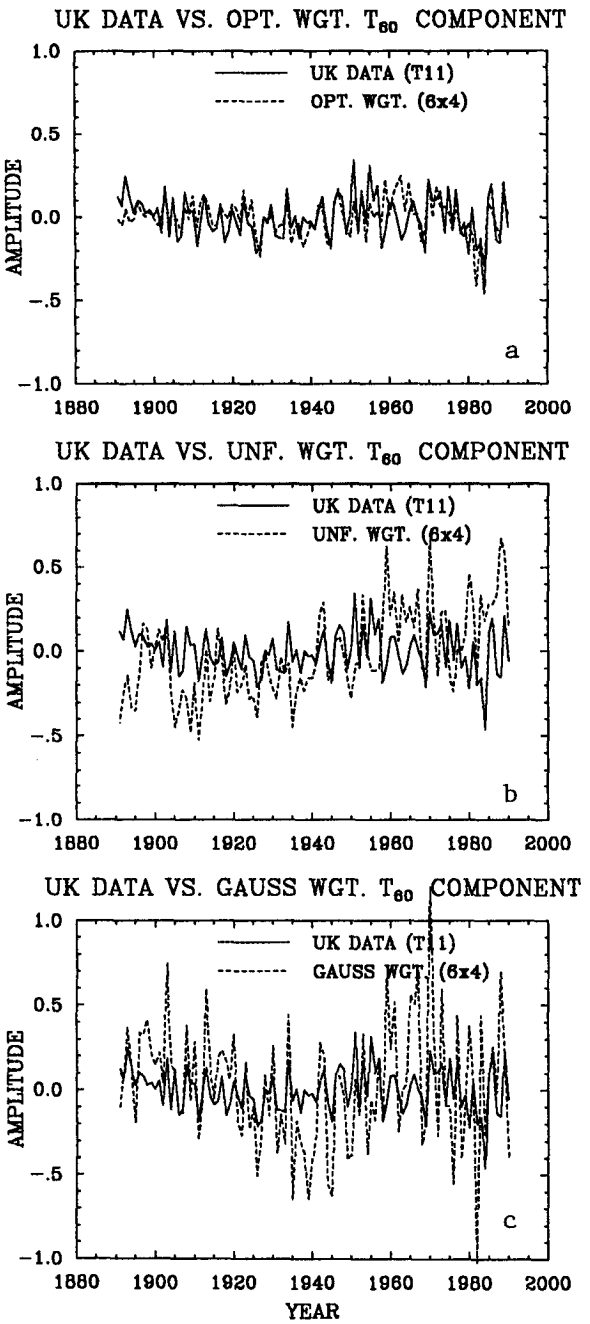

FIG. 5. The 100-yr time series of T_{60} component from the United Kingdom dataset. The estimation technique is based on a 6×4 regular network. Employed weighting schemes are (a) optimal, (b) uniform, and (c) Gaussian. The respective percent sampling errors squared are 42%, 82%, and 85%.

a constant value of $w_j = 4\pi/N_{\text{net}}$. The optimal weighting scheme far excels the uniform weighting scheme. As the number of stations exceeds 200, percent sampling error squared is almost zero for the optimal weighting scheme. For the uniform case, however, there are certain modes for which accuracy of estimation would not improve with the number of stations. In our example, estimate improvement is very sluggish for all the zero-rank modes. This peculiar behavior is due to the neglect of areal weighting. With a proper account

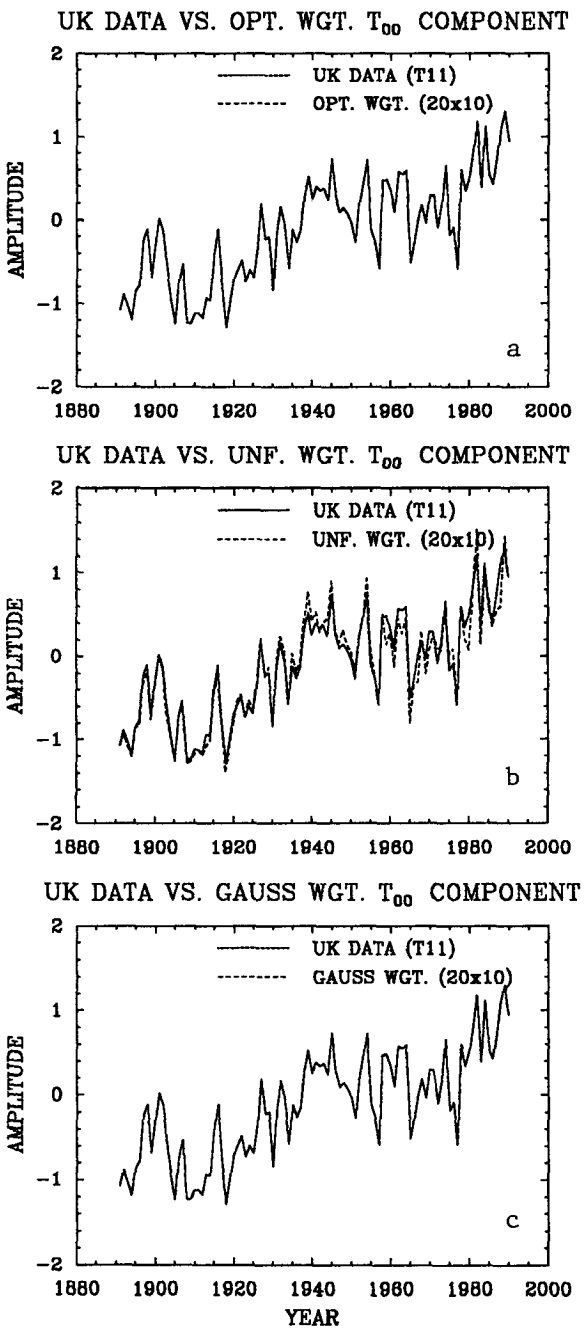

FIG. 6. The 100-yr time series of T_{00} component from the United Kingdom dataset. The estimation technique is based on a 20×10 regular network. Employed weighting schemes are (a) optimal, (b) uniform, and (c) Gaussian. The respective percent sampling errors squared are 0%, 5%, and 0%.

for the areal representation of each quadrature point, as in the Gaussian method below, the estimate should converge to an accurate value with a large number of stations. The optimization of the sampling positions (such as the A–K network) has little effect in the present estimation technique.

We also investigated the percent sampling error for irregular networks (Fig. 2). An irregular network was generated by randomly selecting sampling points with a constraint that the minimum distance with other points is about 7°. If the stations are very close to each other, the matrix problem (15) would be nearly singular and result in large computational error. For a small number of sampling stations, an irregular network performs better than a regular network for the optimal weighting scheme. For such a sparse network, estimation error is large even for the optimal estimator and the fortuitous cancellation of error due to random selection of stations may be more important. As the number of stations exceeds about 50, an irregular network becomes inferior to a regular network. For a dense network one may need to thoroughly cover the observational field without a large gap. Even with 200 sampling stations, percent sampling error squared for an optimal weighting scheme on an irregular network does not approach zero for some modes. For the uniform weighting scheme, however, irregular networks eliminate the estimation inaccuracy associated with zero-rank modes in Fig. 1. These results are robust as shown in the tables below.

Next we consider Gaussian networks. The Gaussian network gauges are at Gaussian points in the meridional direction and are uniformly distributed in the zonal direction. The weights are a set of properly scaled Gaussian weights, which is a function only of latitude. This might be the most popular scheme for computing spherical harmonic coefficients. As shown in Fig. 3, the Gaussian scheme surpasses in performance the uniform weighting scheme because the former accounts for the areal weighting by using an independent variable x (sine of latitude) in its formulation. Also, it is an optimal estimation method in a sense that the result is exact for a polynomial up to a certain degree. It is slightly inferior to the optimal weighting scheme. The Gaussian scheme was not customized for the particular variable we are considering. The Gaussian scheme, however, is difficult to implement for an irregular network.

As a demonstration of practical applicability, we estimated the spherical harmonic coefficients from the 100-yr (1890–1990) United Kingdom dataset. It is a global surface temperature data gridded on a 72 × 36 uniform array. The surface temperatures over land are from Jones et al. (1986a,b), and those over the ocean are from the Comprehensive Ocean–Atmosphere Data Set (Woodruff et al. 1987). Then we calculated the percent sampling error squared based on the assumption that we can calculate true coefficients from a dense

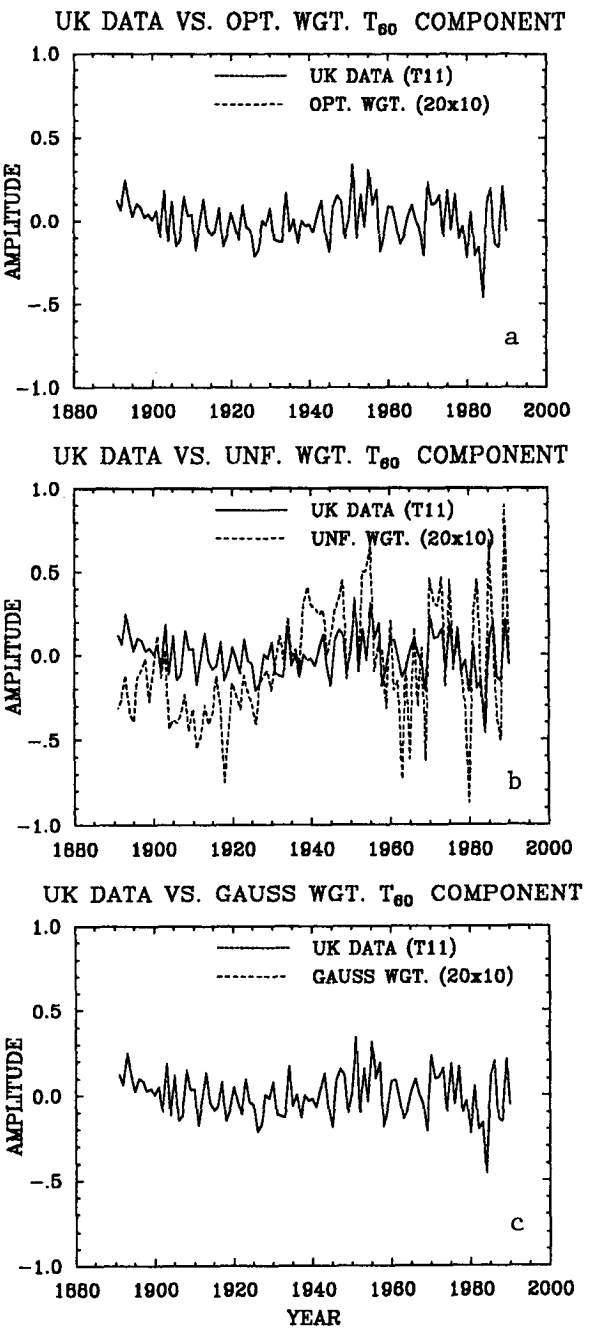

FIG. 7. The 100-yr time series of T_{60} component from the United Kingdom dataset. The estimation technique is based on a 20 × 10 regular network. Employed weighting schemes are (a) optimal, (b) uniform, and (c) Gaussian. The respective percent sampling errors squared are 0%, 83%, and 0%.

(72 × 36) array. Tables 1 and 2 summarize the results of the experiments. The optimal weighting scheme is consistently better than the uniform and Gaussian weighting schemes for both the regular networks (Table 1) and irregular networks (Table 2). The percent

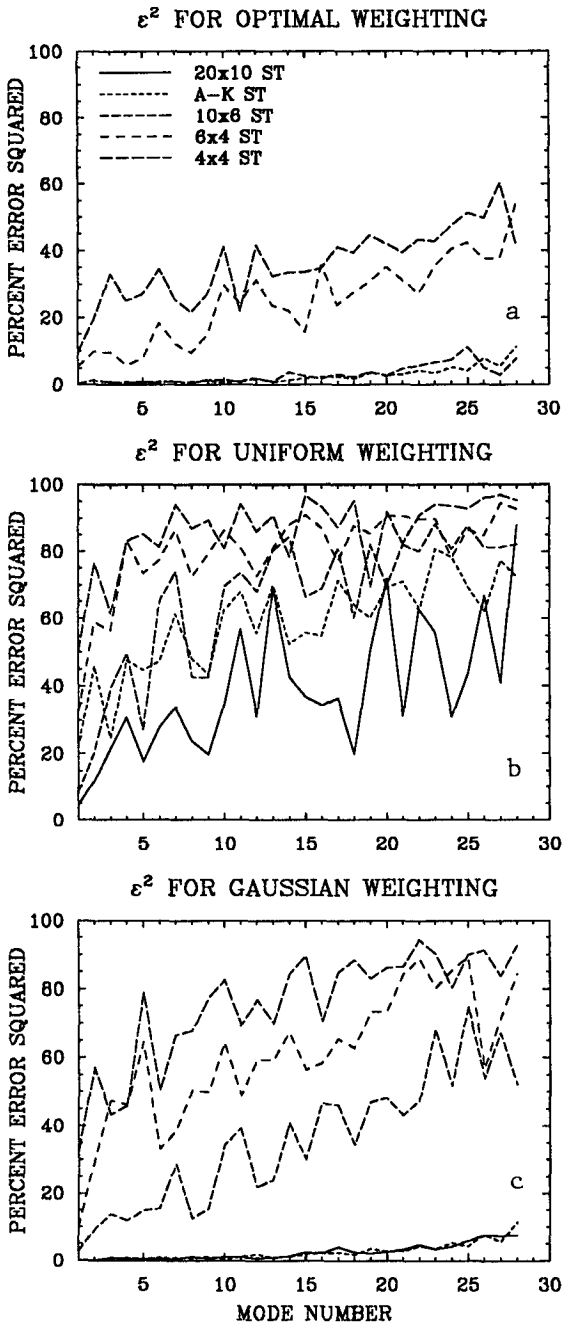

FIG. 8. Percent sampling error squared for four regular networks (20 × 10, 10 × 6, 6 × 4, 4 × 4) and for the Angell–Korshover network. The employed weighting schemes are (a) optimal, (b) uniform, and (c) Gaussian.

sampling error squared obtained from the observation data is very consistent with the theoretical estimation (values in parenthesis).

To better interpret the tables, we plotted a few selected time series. Figures 4 and 5 show, respectively, the time series of T_{00} and T_{60} on a regular 6 × 4 grid. Even with such a sparse network, the optimal weighting scheme does an excellent job. The Gaussian weighting scheme is reasonable for low mode numbers (Fig. 4) but gradually deteriorates with the mode number (Fig. 5). Figures 6 and 7 are the same time series but for a regular 20 × 10 grid. With this large number of gauges, both the optimal and Gaussian weighting schemes do superior jobs. But the uniform weighting scheme does a poor job for certain modes as exemplified in Fig. 7.

Finally, we applied the estimation techniques to calculating the EOF amplitudes. Figure 8 shows the percent sampling error squared for regular networks. Again, the optimal weighting scheme performs best. The uniform weighting scheme introduces large sampling error. The Gaussian scheme improves as the number of gauges is increased but is inferior to the optimal scheme. As shown in Fig. 9, sampling error for the EOF amplitude is not very sensitive to the network configuration. The performance of the estimation schemes at irregular network is comparable to that at regular network.

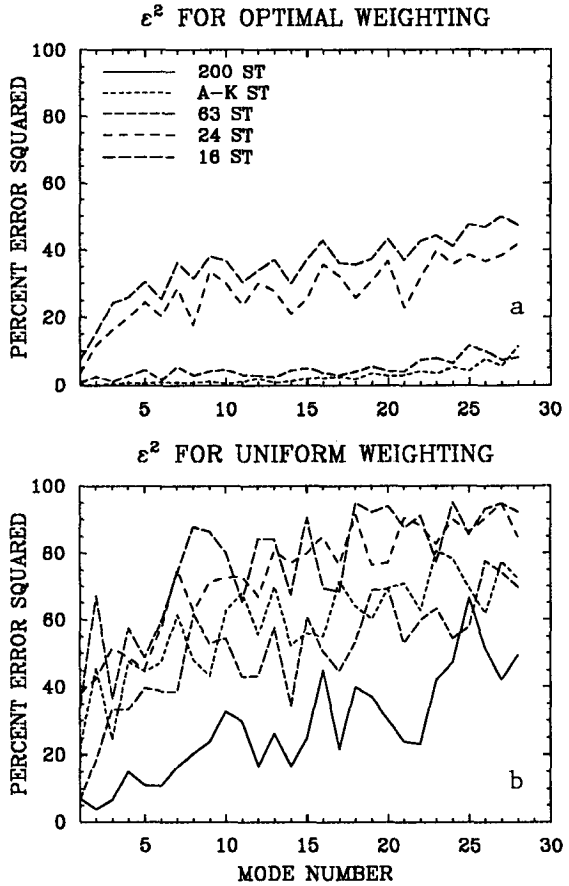

FIG. 9. Percent sampling error squared for four irregular networks (200, 63, 24, 16 points) and for the Angell–Korshover network: (a) optimal weighting scheme, (b) uniform weighting scheme.

4. Summary and concluding remarks

In this study, we implemented an optimal estimation technique for the spherical harmonic coefficients from a network of gauges of certain configuration. The method is based on the variational principle of minimizing least-square error and constitutes computing a set of optimal weights for a given network of gauges. The optimal weights in turn are based on the detailed covariance structure of the field to be estimated, which is represented in terms of EOFs. The optimal estimation technique was tested and was compared with a uniform weighting scheme and a Gaussian weighting scheme to assess the performance of the developed estimation technique. A summary of the results follows.

1) As expected, percent sampling error squared generally decreases with the number of sampling gauges for all the estimation techniques we considered. It tends to increase with the mode number. For an optimal weighting scheme, however, the growth rate of percent sampling error increases slowly with the mode number.

2) The optimal weighting scheme is consistently better than a uniform weighting scheme or a Gaussian scheme. For a small number of sampling gauges (<50), regular and irregular network configurations result in similar performances in an optimal weighting technique. For a large number of stations, a regular network performs better.

3) For a uniform weighting scheme, use of regular networks results in significant sampling errors for certain modes. The performance of the estimation technique improves little for these modes even with a dense network. In our example, all the zero-rank modes were erroneously estimated. For an irregular network, the performance of the uniform weighting scheme improves monotonically with the number of gauges, but the sampling error is still significant even for 200 stations.

4) A Gaussian weighting scheme is much better than a uniform weighting scheme but is inferior to an optimal scheme. It performs well for a given mode if a sufficient number of gauges are available. A remarkable shortcoming of the Gaussian scheme is its large growth rate of percent sampling error squared with the mode number. This implies that for a given number of gauges, there is a rather stringent limitation in the mode numbers that can be estimated accurately. Another deficiency of the scheme is its requirement for a regular network.

5) We validated theoretical estimations of the percent sampling error squared from the observational data. We calculated the percent sampling error squared from a 100-yr United Kingdom dataset. The estimated values are remarkably close to the theoretical limit, thereby demonstrating the utility of the method.

6) For the amplitudes of EOFs, an optimal weighting scheme again performs best. An optimal weighting scheme works well both on regular and irregular networks, and the percent sampling error squared quickly flattens with the mode number and with the number of gauges.

In view of these findings, we feel that the optimal weighting scheme presented here is a useful estimation technique for spherical harmonic coefficients and the amplitudes of EOFs in a spherical harmonic space.

Acknowledgments. We thank the anonymous reviewers for their critical and helpful comments. This research was supported by the Department of Energy via a grant to Texas A&M University through CHAMMP (DE-FG05-91ER61221) and through its Quantitative Links program. The Department of Energy does not necessarily endorse any of the conclusions drawn in the paper.

REFERENCES

Arfken, G., 1985: *Mathematical Methods for Physicists.* 3d ed., Academic Press, 985 pp.

Angell, J. K., and J. Korshover, 1983: Global temperature variations in the troposphere and stratosphere, 1958–1982. *Mon. Wea. Rev.,* **111,** 901–921.

Bell, T. L., 1982: Optimal weighting of data to detect climate change: Application to the carbon dioxide problem. *J. Geophys. Res.,* **87,** 11 161–11 170.

——, 1986: Theory of optimal weighting of data to detect climate change. *J. Atmos. Sci.,* **43,** 1694–1710.

Bourke, W., 1974: A multi-level spectral model. Part I: Formulation and hemispheric integrations. *Mon. Wea. Rev.,* **102,** 687–701.

——, B. McAvaney, K. Puri, and R. Thurling, 1977: Global modeling of atmospheric flow by spectral methods. *General Circulation Methods of the Atmosphere, Methods in Computational Physics,* Vol. 17, J. Chang, Ed., Academic Press, 267–324.

Eliasen, E., B. Machenhauer, and E. Rasmussen, 1970: On a numerical method for integration of the hydrodynamical equations with a spectral representation of the horizontal fields. Rep. No. 2, Institute for Theoretical Meteorology, University of Copenhagen, 35 pp.

Ellsaesser, H. W., 1966: Evaluation of spectral versus grid methods of hemispheric numerical weather prediction. *J. Appl. Meteor.,* **5,** 246–262.

Hardin, J. W., and R. B. Upson, 1993: Estimation of the global average temperature with optimally weighted point gauges. *J. Geophys. Res.,* **98,** 23 275–23 282.

——, G. R. North, and S. S. Shen, 1992: Minimum error estimates of global mean temperature through optimal arrangement of gauges. *Environmetrics,* **3,** 15–27.

Jones, P. D., S. C. B. Raper, R. S. Bradley, H. F. Diaz, P. M. Kelly, and T. M. L. Wigley, 1986a: Northern Hemisphere surface air temperature variations, 1851–1984. *J. Climate Appl. Meteor.,* **25,** 161–179.

——, ——, ——, ——, ——, and ——, 1986b: Southern Hemisphere surface air temperature variations, 1851–1984. *J. Climate Appl. Meteor.,* **25,** 1213–1230.

Kagan, R. L., 1979: *Averaging Meteorological Fields* (in Russian). Gidrometeoizdat, 212 pp.

Kim, K.-Y., and G. R. North, 1991: Surface temperature fluctuations in a stochastic climate model. *J. Geophys. Res.,* **96,** 18 573–18 580.

——, and ——, 1992: Seasonal cycle and second-moment statistics of a simple coupled climate system. *J. Geophys. Res.,* **97,** 20 437–20 448.

——, and ——, 1993: EOF analysis of surface temperature field in a stochastic climate model. *J. Climate,* **6,** 1681–1690.

Madden, R. A., D. J. Shea, G. W. Branstator, J. J. Tribbia, and R. O. Weber, 1993: The effect of imperfect spatial and temporal sampling on estimates of the global mean temperature: Experiments with model data. *J. Climate,* **6,** 1057–1066.

McAvaney, B. J., W. Bourke, and K. Puri, 1978: A global spectral model for simulation of the general circulation. *J. Atmos. Sci.,* **35,** 1557–1538.

North, G. R., S. S. Shen, and J. W. Hardin, 1992: Estimation of the global mean temperature with point gauges. *Environmetrics,* **3,** 1–14.

Orszag, S. A., 1970: Transform method for the calculation of vector-coupled sums: Application to the spectral form of the vorticity equation. *J. Atmos. Sci.,* **27,** 890–895.

Pitcher, E. J., R. C. Malone, V. Ramanathan, M. L. Blackmon, K. Puri, and W. Bourke, 1983: January and July simulations with a spectral general circulation model. *J. Atmos. Sci.,* **40,** 580–604.

Ramanathan, V., E. J. Pitcher, R. C. Malone, and M. L. Blackmon, 1983: The response of a spectral general circulation model to refinements in radiative processes. *J. Atmos. Sci.,* **40,** 605–630.

Shen, S. S., G. R. North, and K-Y. Kim, 1994: Spectral approach to optimal estimation of the global average temperature anomaly. *J. Climate,* **7,** 1999–2007.

——, ——, and ——, 1996: Estimation of the spherical harmonic components of the surface air temperature field. *Environmetrics,* in press.

Trenberth, K. E., and J. G. Olson, 1992: Representativeness of a 63-station network for depicting climate changes. *Greenhouse-Gas-Induced Climatic Change: A Critical Appraisal of Simulations and Observation,* M. Schlesinger, Ed., Elsevier, 249–259.

Vinnikov, K. Ya., P. Ya. Groisman, and K. M. Lugina, 1990: Empirical data on contemporary global climate changes (temperature and precipitation). *J. Climate,* **3,** 662–677.

Williamson, D. L., and P. N. Swarztrauber, 1984: A numerical weather prediction model—computational aspects on the CRAY-1. *Proc. IEEE,* **72,** 56–67.

Woodruff, S. D., R. J. Slutz, R. L. Jenne, and P. M. Steurer, 1987: A Comprehensive Ocean–Atmosphere Data Set. *Bull. Amer. Meteor. Soc.,* **68,** 1239–1250.